Applied Ocean Research 127 (2022) 103325

Contents lists available at ScienceDirect

Applied Ocean Research

journal homepage: www.elsevier.com/locate/apor

Initial stages of a three dimensional dam break flow

Elona Fetahu [a], Olha Ivanyshyn Yaman [b], Oguz Yilmaz [b,*]

[a] Department of Mathematics, University of Elbasan 'Aleksander Xhuvani' 3001, Elbasan, Albania
[b] Department of Mathematics, Izmir Institute of Technology, 35430 Urla, Izmir, Turkey

ARTICLE INFO

Keywords:
Three dimensional dam break flow
Gravity driven free surface flows
Small time asymptotics

ABSTRACT

Short time behavior of a three dimensional, gravity-driven free surface flow is studied analytically and numerically. Initially the fluid is at rest, held by a vertical wall. A rectangular section of the wall suddenly disappears and the gravity driven three-dimensional flow starts. In order to describe the flow in the early stage, the potential theory is employed. Viscous effects are ignored for small times. The leading order problem is solved by using the Fourier series method and an integral equation method. Local analysis of the flow field close to the side edges of the rectangular section reveals a square root singularity. The flow velocity is also log-singular at the bottom edge of the rectangular section. In the limiting case, as the width of the rectangular section approaches infinity, the results of the classical two-dimensional dam break flow are recovered. Three dimensional effects become important closer to the side edges of the rectangular section.

1. Introduction

One of the first investigations into the small time behavior of two dimensional dam break flows is due to Pohle (1950). In the PhD thesis of Pohle, the solution of the gravity-driven flow caused by the collapse of a half-cylinder of fluid was obtained using Lagrangian representation, where the displacement of each particle is determined following each particle while it moves through space and time. The displacements and pressure are expressed in the time power series. Following the same method, Stoker (1957) attempted to solve the problem of two dimensional dam-break flow and discovered a singularity of the vertical free surface shape at the meeting point of the vertical free surface with the bottom. Penney et al. (1952) worked on the collapse of a column of fluid of semicylindrical and hemispherical shapes surrounded by a less dense liquid. The problem was solved using Eulerian representation. They showed that the initial asymptotics of the solution is not valid at the intersection with the bottom. The inner solution near the contact points was not treated in the studies by Penney et al. (1952), Stoker (1957), and Pohle (1950).

There are some experimental investigations on dam-break flows. Among these, the most relevant one to the present paper is the study of Stansby et al. (1998), who undertook some experiments on dam-break flows where a thin vertical plate separating water is withdrawn suddenly in vertical direction. It was observed that at small times a horizontal jet formed at the line where the vertical free surface meets the rigid bed for the dry bed case.

The presence of a jet was also observed by King and Needham (1994) when a uniformly accelerating vertical plate moves into a fluid with a free surface. At the initial intersection of the plate and free surface, the outer solution becomes singular. Near this intersection point matched asymptotic expansions were used to find the inner solution where a jet forms.

Jet formations are also present in the water impact problems at the initial stage. A body's impact on a liquid's free surface was studied by Korobkin and Pukhnachov (1988), where the body has a plane front section. In that paper, it was claimed that the singularity of the velocity field is $r^{-1/2}$ at the vicinity of the contact point, where r is the distance from the contact point. Iafrati and Korobkin (2004) studied the initial stage of the impact of a flat plate with a liquid's free surface. At the plate edges, they discovered a singularity in the liquid's velocity for the leading order outer problem. The inner solution calculations revealed a jet formation at the edges and a square root singularity of the flow velocity.

The experimental and theoretical investigations mentioned above, see Stansby et al. (1998), King and Needham (1994), Korobkin and Pukhnachov (1988) and Iafrati and Korobkin (2004), suggest that mathematical singularity of velocity field near a contact point corresponds to a physical reality in the form of jet formations. The singularities in the linear outer problems mentioned in these studies are caused by the neglect of the fluid inertia. Hence, for the three dimensional problem studied in this paper, jet formations are expected in the regions where a flow singularity is observed.

Many researchers developed numerical methods of dam-break flow by solving the nonlinear shallow water equations (SWE) (Brufau et al.,

* Corresponding author.
E-mail addresses: elona.fetahu@uniel.edu.al (E. Fetahu), ivanyshynyaman@iyte.edu.tr (O.I. Yaman), oguzyilmaz@iyte.edu.tr (O. Yilmaz).

https://doi.org/10.1016/j.apor.2022.103325
Received 31 May 2022; Received in revised form 9 August 2022; Accepted 18 August 2022
Available online 5 September 2022

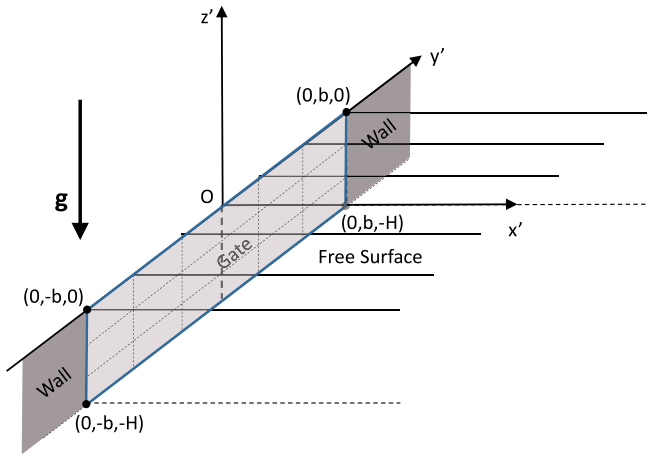

Fig. 1. Flow region at initial time $t' = 0$.

2002; Jha et al., 1995; Zhou et al., 2004; Issakhov and Mussakulova, 2017). These models are useful in predicting the flooding depth but they are not adequate for predicting some hydraulic aspects, especially at the initial stages of dam break flow. During a short time period after the dam break, the flow is mainly due to gravity and the hydrostatic pressure distribution is not valid (Biscarini et al., 2010).

In recent years, some researchers attempted to solve the full Navier Stokes equations for the dam break flow, thanks to recent advances in high performance computers (Larocque et al., 2013; Issakhov et al., 2018; Caboussat et al., 2011). Caboussat's model is based on the incompressible Navier Stokes equations coupled with a volume-of-fluid approach. Several numerical experiments including two benchmark problems and two real-life situations were carried out and it was concluded that the three dimensional effects are important where the fluid velocities are discontinuous. It was also mentioned that three dimensional (3D) numerical simulations are very expensive and that simplified models remain useful.

In this paper, three dimensional effects of a dam break flow are investigated. Viscous effects are assumed to be negligible for small times and ignored, see Fetahu and Yilmaz (2021) for details. It is found that the velocity of the outer solution at the bottom line of the rectangular section is singular and a jet formation is expected, which is similar to that in the classical dam break problem (Korobkin and Yilmaz, 2009). In the limiting case in which the horizontal length of the rectangular section approaches infinity, the problem reduces to the classical two dimensional dam break problem (dry bed case). It is concluded that three dimensional effects are important close to the vertical edges of the rectangular section, where a singularity in the velocity field of the outer solution stronger than the logarithmic singularity at the bottom line is suspected.

In Section 2 the problem is formulated assuming that the fluid is inviscid and incompressible. The leading order solution is simplified in Section 3 by separating the dependence on the vertical coordinate and a singularity analysis is carried out in this section. The numerical boundary element method used is described in Section 4. The results are discussed in Section 5.

2. Formulation of the problem

A rectangular section of a wall that holds a certain liquid with a free surface suddenly disappears and the flow starts under the effect of gravity. The problem is unsteady and three dimensional. Eulerian variables are used to determine the nature of the flow for short times. At $t' = 0$ the fluid is at rest and its domain is the region $\Omega'(x', y', z', 0)$: $x' > 0, -\infty < y' < \infty, -H \le z' \le 0$, which is held in its place by a wall in the shape of an infinite strip $x' = 0, -\infty < y' < \infty, -H \le z' \le 0$ and by a rigid bottom, $z' = -H$, where H is the liquid depth and a prime stands for dimensional variables. At $t' = 0$ the rectangular section of the wall ("the gate"), $x' = 0, -b \le y' \le b, -H \le z' \le 0$, suddenly disappears The rectangular coordinate system (x', y', z') is placed at the free surface with the upward orientation for z' axis (see Fig. 1). The liquid is assumed inviscid and incompressible. The resulting flow is potential and symmetric with respect to the $x'z'$ plane. The governing equation for the velocity potential $\phi'(x', y', z', t')$ is the Laplace's equation

$$\nabla^2\phi' = 0 \text{ in } \Omega'(t'), \tag{1}$$

where $\Omega'(x', y', z', t')$ is the flow region.

The free surface of the domain, $FS'(t')$, consists of two parts: the initially horizontal free surface which is infinite in extent, $FS'_h(t')$, and the initially vertical free surface $FS'_v(t')$ which is finite in extent,

$$FS'_h(t') = \{(x', y', z', t') \mid z' = \eta'(x', y', t'), x' > h'(y', \eta', t'), -\infty < y' < \infty\},$$

$$FS'_v(t') = \{(x', y', z', t') \mid x' = h'(y', z', t'), -H < z' < \eta'(h', y', t'), -b < y' < b\}.$$

Boundary conditions are imposed on the free surfaces, at the rigid bed and at infinity. The dynamic free surface condition implies that the fluid pressure p' is atmospheric at the free surface,

$$p' = 0 \text{ in } FS'(t'), \tag{2}$$

where atmospheric pressure is taken as the reference pressure. The kinematic free surface conditions, state that the fluid particles that are at the free surface at $t' = 0$ remain there,

$$\phi'_{z'} - \phi'_{x'}\eta'_{x'} - \phi'_{y'}\eta'_{y'} - \eta'_{t'} = 0 \text{ at } FS'_h(t'), \tag{3}$$

$$\phi'_{x'} - \phi'_{y'}h'_{y'} - \phi'_{z'}h'_{z'} - h'_{t'} = 0 \text{ at } FS'_v(t'). \tag{4}$$

There is the slip boundary condition at the rigid bottom,

$$\phi'_{z'} = 0 \text{ at } z' = -H. \tag{5}$$

Finally the condition at infinity is imposed, which implies that the effects of dam break are not felt at ∞,

$$\phi' \to 0 \text{ as } (x')^2 + (y')^2 \to \infty. \tag{6}$$

Also, it is imposed that the fluid is at rest initially,

$$\phi'(x', y', z', 0) = 0,\ \eta'(x', y', 0) = 0,\ h'(y', z', 0) = 0, \tag{7}$$

$$p'(x', y', z', 0) = -\rho_0\, g z'.$$

Bernoulli's equation for unsteady irrotational flow is employed to relate the fluid pressure $p'(x', y', z', t')$ to the velocity potential

$$\frac{p'}{\rho_0} + \frac{\partial\phi'}{\partial t'} + \frac{1}{2} \mid \nabla\phi' \mid^2 + g z' = 0,$$

in the fluid domain, where g is the gravitational acceleration and ρ_0 is the fluid density.

In order to nondimensionalize the problem, dimensionless unprimed variables are introduced,

$$x' = Hx,\ y' = Hy,\ z' = Hz,\ t' = Tt,\ \phi' = gHT\phi,\ p' = \rho_0 g H p,$$
$$T = \epsilon^{1/2}\sqrt{H/g},$$

where ϵ is a small dimensionless parameter which indicates that we are dealing with the initial stage of the flow in which $\epsilon \to 0$.

The problem (1)–(7) is expressed in dimensionless form,

$$\nabla^2\phi = 0 \text{ in } \Omega(t), \tag{8}$$

$$p = 0 \text{ on } FS(t), \tag{9}$$

$$\phi_z - \epsilon\phi_x\eta_x - \epsilon\phi_y\eta_y - \eta_t = 0 \text{ on } FS_h(t), \tag{10}$$

$$\phi_x - \epsilon\phi_y h_y - \epsilon\phi_z h_z - h_t = 0 \text{ on } FS_v(t), \tag{11}$$

$$\phi_z = 0 \text{ at } z = -1, \tag{12}$$

$$\phi \to 0 \text{ as } r \to \infty, \tag{13}$$

$$\phi(x,y,z,0) = 0,\ \eta(x,y,0) = 0,\ h(y,z,0) = 0,\ p(x,y,z,0) = -z, \tag{14}$$

where $\Omega(x,y,z,t)$ is the fluid domain and $FS(t)$ is the free surface composed by the horizontal free surface $FS_h(t)$ and the vertical free surface $FS_v(t)$,

$$FS(t) = FS_h(t) \cup FS_v(t),$$

$$FS_h(t) = \{(x,y,z,t) \mid z = \epsilon\eta(x,y,t), x > \epsilon h(y,\epsilon\eta,t), -\infty < y < \infty\},$$

$$FS_v(t) = \{(x,y,z,t) \mid x = \epsilon h(y,z,t), -1 < z < \epsilon\eta(\epsilon h,y,t), -b/H < y < b/H\}.$$

The Bernoulli equation in dimensionless form becomes,

$$p + \frac{\partial\phi}{\partial t} + \frac{1}{2}\epsilon \mid \nabla\phi \mid^2 + z = 0,$$

in the fluid domain.

The following asymptotic expansions for the unknown variables ϕ, η and h are suggested for small times,

$$\phi(x,y,z,t,\epsilon) = \phi_0(x,y,z,t) + \epsilon\phi_1(x,y,z,t) + O(\epsilon^2), \tag{15}$$

$$\eta(x,y,t,\epsilon) = \eta_0(x,y,t) + \epsilon\eta_1(x,y,t) + O(\epsilon^2),$$

$$h(y,z,t,\epsilon) = h_0(y,z,t) + \epsilon h_1(y,z,t) + O(\epsilon^2),$$

as $\epsilon \to 0$.

3. The leading order problem

The asymptotic expansions (15) are substituted in the problem (8)–(14) and the leading order problem is obtained as $\epsilon \to 0$,

$$\nabla^2\phi_0 = 0 \ (x > 0, -\infty < y < \infty, -1 < z < 0), \tag{16a}$$

$$\phi_0 = 0,\ \phi_{0,z} = \eta_{0,t} \ (x > 0, -\infty < y < \infty, z = 0), \tag{16b}$$

$$\phi_0 = -zt,\ \phi_{0,x} = h_{0,t} \ (x = 0, -b/H < y < b/H, -1 < z < 0), \tag{16c}$$

$$\phi_{0,x} = 0 \ (x = 0, |y| > b/H, -1 < z < 0), \tag{16d}$$

$$\phi_{0,z} = 0 \ (x > 0, -\infty < y < \infty, z = -1), \tag{16e}$$

$$\phi_0 \to 0 \ (x^2 + y^2 \to \infty), \tag{16f}$$

$$\phi_0(x,y,z,0) = 0,\ \eta_0(x,y,0) = 0,\ h_0(y,z,0) = 0. \tag{16g}$$

First equation in (16c) is the dynamic boundary condition on the vertical free surface, while the second one is the kinematic condition. The former implies that dynamic pressure balances hydrostatic pressure on the initially vertical free surface. Note that, on the gate, the velocity in z direction is $\frac{\partial\phi_0}{\partial z} = -t$ (See (16c)) which is also true approaching the lower horizontal line of the gate as $z \to -1^+$. However, from (16e) we calculate that the velocity in z direction is zero at the rigid bottom, $z = -1$. That means that the boundary conditions (16c) and (16e) do not match each other at the bottom line $x = 0, -b/H < y < b/H, z = -1$, which is a sign of irregularity.

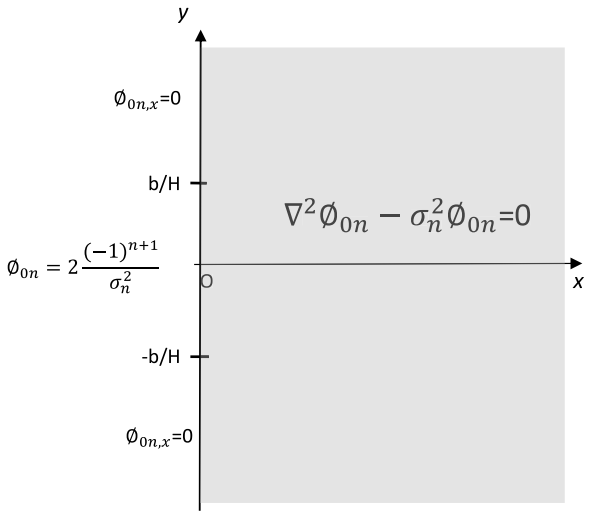

Fig. 2. Boundary Value Problem for ϕ_{0n} on the right half plane together with the condition that ϕ_{0n} vanishes at infinity.

The solution to the boundary value problem (16) is sought by first separating the z dependence (See Eq. (17) of Renzi and Dias, 2013),

$$\phi_0(x,y,z,t) = t\sum_{n=0}^{\infty}\phi_{0n}(x,y)\sin(\sigma_n z), \tag{17}$$

where

$$\sigma_n = \frac{\pi}{2}(2n+1),\ n = 0,1,\ldots.$$

Eq. (17) satisfies the Laplace's Eq. (16a), the dynamic free surface condition on $z = 0$ (16b), the slip boundary condition at the rigid bottom $z = -1$ (16e) and the initial condition (16g). By plugging in the suggested form of the velocity potential (17) in the boundary value problem (16) and using the orthogonality of the sine function, we arrive at the following problem for the function $\phi_{0n}(x,y)$ on the half plane, $x > 0$, (See Fig. 2),

$$\nabla^2\phi_{0n} - \sigma_n^2\phi_{0n} = 0 \ (x > 0, -\infty < y < \infty), \tag{18a}$$

$$\phi_{0n}(0,y) = 2\frac{(-1)^{n+1}}{\sigma_n^2} \ (x = 0, -b/H < y < b/H), \tag{18b}$$

$$\phi_{0n,x} = 0 \ (x = 0, |y| > b/H), \tag{18c}$$

$$\phi_{0n}(x,y) \to 0 \text{ as } (x^2 + y^2) \to \infty. \tag{18d}$$

In the limiting case as $b/H \to \infty$, the three dimensional dam break problem becomes two dimensional and we should be able to recover the results given in Korobkin and Yilmaz (2009). In this limiting case the boundary condition (18b) is now on the whole of y axis, there is no y dependence of the function ϕ_{0n} and the solution of the boundary value problem (18) is

$$\phi_{0n}(x,y) \sim 2\frac{(-1)^{n+1}}{\sigma_n^2}\exp(-\sigma_n x) \text{ as } b/H \to \infty. \tag{19}$$

If the representation (19) is substituted in (17) the leading order solution is obtained

$$\phi_0(x,y,z,t) \sim 2t\sum_{n=0}^{\infty}\frac{(-1)^{n+1}}{\sigma_n^2}\exp(-\sigma_n x)\sin(\sigma_n z), \tag{20}$$

as $b/H \to \infty$. Eq. (20) is the same as Eq. (12) of Korobkin and Yilmaz (2009), which is the leading order solution of the classical two dimensional dam break problem.

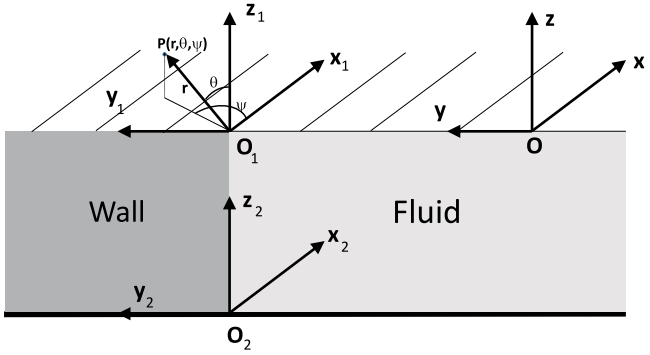

Fig. 3. New coordinate axes at the corner points $(0, b/H, 0)$ and $(0, b/H, -1)$.

Two other interesting limiting cases involve the behavior of the fluid near the corner points of the gate. Let us start with one of the top corner points. A new coordinate system (x_1, y_1, z_1)

$$x_1 = x, y_1 = y - b/H, z_1 = z$$

is placed at the top corner point $(0, b/H, 0)$. Hence, we consider the vicinity of the point $(0, b/H, 0)$ (See Fig. 3). Spherical coordinates (r, θ, ψ)

$$x_1 = r\sin\theta\cos\psi, y_1 = r\sin\theta\sin\psi, z_1 = r\cos\theta, \tag{21}$$

where ψ is the azimuthal angle, are employed to write the boundary value problem near the top corner point as

$$\nabla^2\phi_0 = 0 \ (r \geq 0, \pi/2 \leq \theta < \pi, -\pi/2 \leq \psi \leq \pi/2), \tag{22a}$$

$$\phi_0 = 0 \ (r \geq 0, \theta = \pi/2, -\pi/2 \leq \psi \leq \pi/2), \tag{22b}$$

$$\phi_0 = -tr\cos\theta \ (r \geq 0, \psi = -\pi/2, \pi/2 \leq \theta < \pi), \tag{22c}$$

$$\phi_{0,x_1} = \phi_{0,\psi} = 0 \ (r \geq 0, \psi = \pi/2, \pi/2 \leq \theta < \pi). \tag{22d}$$

By separating the variables we arrive at the solution

$$\phi_0 \sim -tr\cos\theta + Ar^{1/2}P_{1/2}^{1/2}(\cos\theta)\cos\left(\frac{\psi}{2} - \frac{\pi}{4}\right), \tag{23}$$

$(r \geq 0, \pi/2 \leq \theta < \pi, -\pi/2 \leq \psi \leq \pi/2)$

where A is a constant which depends on the global flow and $P_{1/2}^{1/2}(\cos\theta)$ is an associated Legendre function of the first kind (See Abramowitz and Stegun, 1970, p. 334, formula 8.6.12),

$$P_{1/2}^{1/2}(\cos\theta) = (\frac{1}{2}\pi)^{-1/2}(\sin\theta)^{-1/2}\cos\theta.$$

Note that ϕ_0 given by (23) is continuous in r, $(r \geq 0)$, but not continuous with respect to θ when $\theta = \pi$. In fact ϕ_0 has an infinite discontinuity at $\theta = \pi$. For this reason the line, $\theta = \pi$, which corresponds to the vertical edge of the rectangular section, is not included in the domain of the function ϕ_0. The fluid velocity normal to the gate can be calculated by differentiating (23),

$$\phi_{0,x} \sim \frac{A}{2}\frac{P_{1/2}^{1/2}(\cos\theta)}{\sin\theta}\frac{1}{r^{1/2}}, \tag{24}$$

as $r \to 0$, $\psi = -\frac{\pi}{2}$ and for a fixed angle θ where $\pi/2 \leq \theta < \pi$. Eq. (24) shows that the leading order horizontal velocity is singular at the order $r^{-1/2}$ on the gate approaching the top corner points. The cause of the singularity is the discontinuous horizontal velocity field near the side lines of the gate, $y = \pm b/H, -1 < z < 0$; on the wall front of the side lines, $\psi = \pi/2, \pi/2 \leq \theta < \pi$, velocity normal to the wall is zero (slip condition), whereas on the other front (on the gate), $\psi = -\pi/2, \pi/2 \leq \theta < \pi$, normal velocity is, physically, a finite non-zero value. In fact the discontinuous velocity field exists all along the sidelines of the gate, so the leading order horizontal velocity is singular, within the linear mathematical considered, at the order $r^{-1/2}$ on the gate approaching the side lines of the gate.

The singularity analysis at the bottom corner points of the gate is quite interesting: if we approach one of these corner points, say the one on the left, along the side line $y = b/H$, $-1 < z < 0$ the flow singularity is $r^{-1/2}$ as demonstrated in the previous paragraph, however if we approach that point along the bottom line the singularity is logarithmic as shown in Section 5. To understand what happens to the flow when approaching this point in an oblique angle a new coordinate system (x_2, y_2, z_2)

$$x_2 = x, y_2 = y - b/H, z_2 = z + 1$$

is placed at the corner point $(0, b/H, -1)$. Hence, we consider the vicinity of the point $(0, b/H, -1)$ (See Fig. 3). Spherical coordinates $(\tilde{r}, \tilde{\theta}, \tilde{\psi})$

$$x_2 = \tilde{r}\sin\tilde{\theta}\cos\tilde{\psi}, y_2 = \tilde{r}\sin\tilde{\theta}\sin\tilde{\psi}, z_2 = \tilde{r}\cos\tilde{\theta}, \tag{25}$$

where $\tilde{\psi}$ is the azimuthal angle, are employed to write the boundary value problem near the bottom corner point as

$$\nabla^2\phi_0 = 0 \ (\tilde{r} > 0, 0 < \tilde{\theta} < \pi/2, -\pi/2 < \tilde{\psi} < \pi/2), \tag{26a}$$

$$\phi_{0,x_2} = 0 \ (r > 0, \tilde{\psi} = \pi/2, 0 < \tilde{\theta} < \pi/2), \tag{26b}$$

$$\phi_0 = -t(z_2 - 1) \ (r > 0, \psi = -\pi/2, 0 < \theta < \pi/2), \tag{26c}$$

$$\phi_{0,z_2} = 0 \ (r > 0, \theta = \pi/2, -\pi/2 < \psi < \pi/2). \tag{26d}$$

As was done for the upper corner point, by separating the variables we arrive at the solution

$$\phi_0 \sim t - tr\cos\theta + Br^{-1/2}P_{-1/2}^{1/2}(\cos\theta)\cos\left(\frac{\psi}{2} - \frac{\pi}{4}\right), \tag{27}$$

where $P_{-1/2}^{1/2}(\cos\theta)$ is an associated Legendre function of the first kind (See Abramowitz and Stegun, 1970, p. 334, formula 8.6.12),

$$P_{-1/2}^{1/2}(\cos\theta) = (\frac{1}{2}\pi)^{-1/2}(\sin\theta)^{-1/2}.$$

Fluid velocity normal to the gate can be calculated as

$$\phi_{0,x} \sim \frac{B}{2}\frac{P_{-1/2}^{1/2}(\cos\theta)}{\sin\theta}\frac{1}{r^{3/2}}, \ r \to 0, \psi = -\frac{\pi}{2}, -\frac{\pi}{2} < \theta < 0, \tag{28}$$

where the constant B depends on the global flow. As is seen from (28), the flow near the bottom corner point is more singular, at the order of $r^{-3/2}$, than the square root singularity at the vertical side $y = b/H$ and the logarithmic singularity at the bottom line $z = -1$ of the gate. An inner solution near the side and bottom lines of the gate could be sought. The inner region problem is quite difficult because it is three dimensional and it involves three different types of singularity at the edge lines and the corner points of the gate. In this paper we do not attempt the inner region problem.

4. Solution of the boundary value problem (18) by an integral equation method

The boundary value problem (18) is difficult to solve by analytical methods. In this section we attempt to solve it by a numerical method based on Green's function technique. The fundamental solution for the modified Helmholtz Eq. (18a) is (See equation 7.2.18, Morse and Feshbach, 1953)

$$\frac{1}{2\pi}K_0(\sigma_n \mid \mathbf{x} - \mathbf{x_0} \mid),$$

where $K_0(x)$ is the modified Bessel function of second kind of order zero, $\mathbf{x} = (x, y)$ is a field point and $\mathbf{x_0} = (x_0, y_0)$ is a source point. The

image method is used to obtain the Green's function for the half plane $x > 0$

$$G(\mathbf{x}, \mathbf{x_0}) = \frac{1}{2\pi} K_0(\sigma_n \mid \mathbf{x} - \mathbf{x_0} \mid) + \frac{1}{2\pi} K_0(\sigma_n \mid \mathbf{x} - \mathbf{x_0^*} \mid), \tag{29}$$

where $\mathbf{x_0^*} = (-x_0, y_0)$. The Green's function (29) satisfies the condition that its normal derivative is zero on y axis and vanishes at infinity.

Green's second formula is used to form an integral equation for the x derivative of the function ϕ_{0n} on the line segment $x = 0, |y| < b/H$,

$$\iint_D \left(\phi_{0n}\nabla^2 G - G\nabla^2\phi_{0n}\right) dA = \oint_C \left(\phi_{0n}\nabla G - G\nabla\phi_{0n}\right) \cdot \mathbf{n} ds, \tag{30}$$

where C is the union of a line segment $[-R, R]$ on the y axis and the semicircle, $x^2 + y^2 = R^2, x > 0$ and D is the region bounded by C. As R approaches infinity, D becomes the right half plane (See Fig. 2). By using (30), the boundary value problem (18) and the properties of the Green's function, the following equation is obtained,

$$-\phi_{0n}(\mathbf{x}) = \int_{-b/H}^{b/H} G(\mathbf{x}, \mathbf{x_0}) \frac{\partial}{\partial x_0} \phi_{0n}(\mathbf{x_0}) dy_0, \; y \in [-b/H, b/H], \tag{31}$$

where $\mathbf{x}$ is a point on the boundary, $x_0 = 0$ on the right hand side under the integral sign and the Green's function $G(\mathbf{x}, \mathbf{x_0})$ on y axis is simplified to be

$$G(\mathbf{x}, \mathbf{x_0}) = \frac{1}{\pi} K_0\left(\sigma_n \sqrt{x^2 + (y - y_0)^2}\right). \tag{32}$$

Note that Eq. (31) is a Fredholm integral equation of the first kind in the unknown variable $\frac{\partial}{\partial x_0}\phi_{0n}$ with $-b/H < y < b/H$.

For the numerical calculations, the line segment $[-b/H, b/H]$ is partitioned into linear panels and the unknown function $\frac{\partial}{\partial x_0}\phi_{0n}$ is assumed to be constant within each panel. Hence the integral Eq. (31) is written in the discrete form

$$-\left(\phi_{0n}\right)_i = \sum_{j \in Q} (g)_{ij} \left(\phi_{0n,x_0}\right)_j, \; i \in Q, \tag{33}$$

where Q is the set of linear panels used to partition the line segment $[-b/H, b/H]$, $\left(\phi_{0n}\right)_i$ and $\left(\phi_{0n,x_0}\right)_i$ denote the values of the velocity potential ϕ_{0n} and its derivative respectively at the mid point of the panel i. The Green's function $G(\mathbf{x}, \mathbf{x_0})$ is integrated along the length of each panel and its value is denoted by $(g)_{ij}$,

$$(g)_{ij} = \frac{1}{\pi} \int_{a_j - l_j}^{a_j + l_j} K_0\left(\sigma_n \sqrt{x_i^2 + (y_i - y_{0j})^2}\right) dy_{0j}, \tag{34}$$

where a_j is the mid point and $2l_j$ is the length of the panel j. Care is taken with the integration in (34), i.e., about the logarithmic singularity, when the field point coincides with the source point, that is, when $i = j$ (See Battistin and Iafrati, 2003).

The discretization of the line segment $[-b/H, b/H]$ is done in such a way that the closer the distance to the edges, the denser the panels. This procedure is described in Yilmaz et al. (2013) and the reason for it is that closer to the edges of the line segment $[-b/H, b/H]$ a singularity is expected and the numerical results support this view.

5. Numerical results and discussion

The flow velocity normal to the gate is calculated by differentiating the velocity potential ϕ_0 in (17) with respect to x at $x = 0$ and truncating the infinite series,

$$\phi_{0,x}(0, y, z, t) = t \sum_{n=0}^{M} \phi_{0n,x}(0, y) \sin(\sigma_n z), \tag{35}$$

where $-b/H < y < b/H, -1 < z < 0$ and the x derivative of the potential ϕ_{0n} is calculated at discrete values of y using (33). Eq. (35) provides the velocity normal to the gate at various points of the gate.

The convergence of the truncated series for the normal velocity (35) is investigated numerically in Tables 1 and 2, where $H = 1$ and $b = 0.5$.

It is observed from Table 1 that the convergence of the horizontal velocities is generally quite good at the vertical line $y = 0$ at the gate. The velocities are increasing at the points that are very close to the bottom, where a logarithmic singularity is expected. Along the horizontal line $z = -0.49899$ at the gate (see Table 2), which is almost the halfway between the bottom $z = -1$ and the free surface $z = 0$, the convergence is fine but the velocities are quite large closer to the edge $y = 0.5$, which could be a sign for a singularity on the line $y = b/H$. This last point about a possible singularity along the edges $y = \pm 0.5$ is shown analytically in Section 3 and will be investigated further numerically.

Table 1
Convergence of the horizontal velocities $\phi_{0,x}$ at various points on the line $y = 0$.

z : M	100	150	200	250
−0.506	−0.6872	−0.6895	−0.6874	−0.6881
−0.750	−1.1731	−1.1748	−1.1778	−1.1774
−0.900	−1.7655	−1.7603	−1.7632	−1.7614
−0.975	−2.6662	−2.5981	−2.6179	−2.6242
−0.999	−4.0187	−4.1512	−4.2184	−4.2554

Table 2
Convergence of the horizontal velocities $\phi_{0,x}$ at various points on the line $z = -0.49899$.

y : M	100	150	200	250
0	−0.6796	−0.6756	−0.6776	−0.6765
0.1970	−0.7535	−0.7487	−0.7513	−0.7498
0.4020	−1.1100	−1.1039	−1.1077	−1.1052
0.4970	−5.8993	−5.8922	−5.8967	−5.8936
0.4990	−10.2266	−10.2180	−10.2231	−10.2197
0.4995	−14.5423	−14.5315	−14.5376	−14.5337
0.4999	−33.1672	−33.1455	−33.1573	−33.1501

The observation of the logarithmic singularity at the lower line of the gate and the square root singularity in the leading order velocity at the side lines of the gate (Eq. (24)) are verified in Fig. 4. The red dot-curves on Fig. 4 correspond to the data presented in the column $M = 200$ of Tables 1 and 2, respectively. It is illustrated on Fig. 4(a) that the flow singularity at the bottom of the gate is logarithmic. As far as the singularity along the edges $y = \pm b/H$ is concerned (See Fig. 4b), the three dimensional dam break problem is similar to the water impact problem of a flat body, which has the singular velocity field $r^{-1/2}$ near the contact point, where r is the distance from the contact point (Korobkin and Pukhnachov, 1988). Hence it is shown analytically and numerically that the singularity in the velocity field of the outer solution near the edges $y = \pm b/H$ is $r^{-1/2}$. It is concluded that three dimensional effects become important closer to the vertical edges of the gate.

It is useful to plot the normal velocity along the horizontal lines (z = constant), along the vertical lines (y = constant) and on a grid on the gate. We start with normal velocities on vertical lines, Figs. 5 and 6. The horizontal velocity along the vertical lines, y = constant, on the gate allows a check on the validity of the method used: along the central vertical line $y = 0$ the flow should be similar to the two dimensional classical dam break flow and furthermore as the length of the gate becomes larger, $b \to \infty$, the flow should be identical to that of the two dimensional problem. This is indeed the case (see Fig. 5) and it is safe to conclude that the singularity at the horizontal bottom line of the gate is logarithmic. To investigate convergence for different b/H, the discretization near the endpoints is kept the same as in the smallest value of b/H, the interior region is discretized in an equidistant manner.

Fig. 6(a) shows the horizontal velocity along the vertical lines, y = constant, and it is seen that closer to the edges $y = \pm b/H$ the velocities become quite large indicating a singularity at the edges stronger than the logarithmic singularity at the bottom line $z = -1$, which will be validated by considering the velocities along the horizontal lines with $M = 200$.

The velocity normal to the gate along the horizontal lines, z = constant, on the gate is shown in Fig. 6(b). It is observed that closer to the edges $\pm b/H$, the velocity becomes larger and larger, which

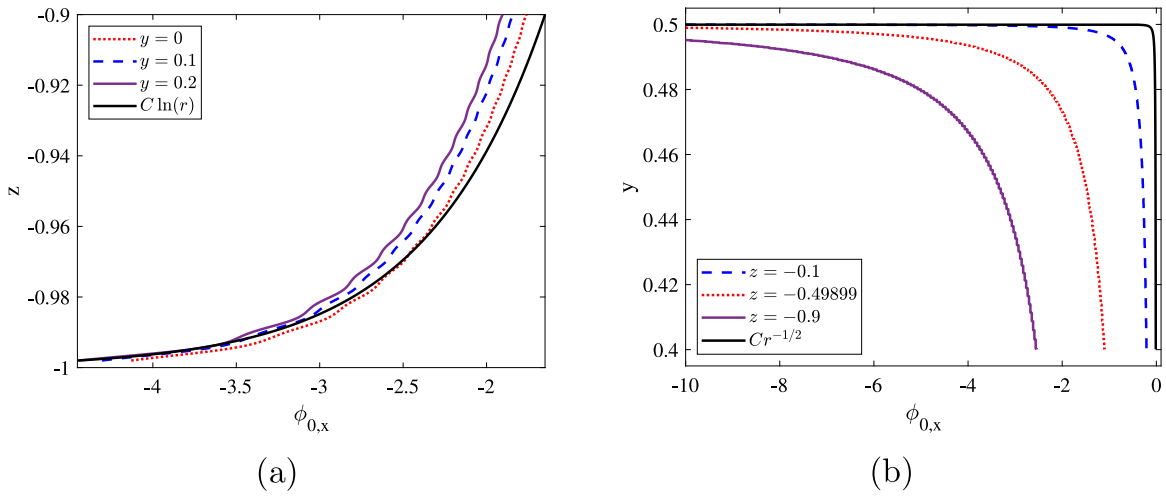

Fig. 4. Horizontal velocities for $x = 0$, $b/H = 0.5$, $t = 1$ (a) approaching the bottom line of the gate, (b) approaching the side line of the gate.

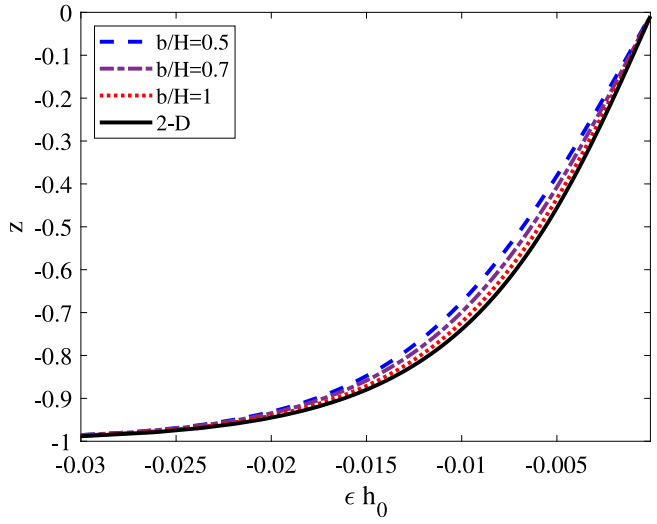

Fig. 5. The shape of the free surface at $y = 0$ for different values of b/H, $\epsilon = 0.01$, $t = 1$.

validates the singularity at the edges within the mathematical model considered in this paper. Fig. 6 suggests that the singularity at the edges $y = \pm b/H$ is stronger than the logarithmic singularity at the bottom line $z = -1$. Finally a grid is formed on the gate with horizontal and vertical lines and the velocities are calculated and plotted along these lines so that a three dimensional picture of the flow is obtained in Fig. 7.

6. Conclusions

The small-time behavior of a three dimensional dam break flow, in which a section of the wall collapses, is studied analytically and numerically. A leading order solution is obtained by first separating the dependence on the vertical coordinate and then using an integral equation method. Two limiting cases are studied: (1) as the breadth to the depth ratio (b/H) becomes larger two dimensional classical dam break flow results are recovered, (2) near the vertical edges of the gate, ($y = \pm b/H, 0 < z < -1$), the outer fluid flow is found to be singular at the order $r^{-1/2}$ within the linear mathematical considered.

Numerical results verify that the flow along the vertical central line of the gate, $y = 0$, is very similar to that of the classical two dimensional dam break problem with logarithmic singularity at the bottom point ($y = 0, z = -1$) and that as the breadth to the depth ratio becomes larger the flow along the central line becomes identical to that of the two dimensional problem.

It is observed analytically and numerically that the singularity in the fluid flow at the side edges of the gate, ($y = \pm b/H$), is stronger than the logarithmic one at the bottom line of the gate, ($z = -1$). This singularity in the fluid flow at the side edges of the gate is at the order of $r^{-1/2}$, which is similar to the one in the water impact problems. It is concluded that three dimensional effects become important closer to the vertical edges of the gate.

There are three types of singularity in the leading order fluid flow: logarithmic singularity at the bottom line $z = -1$ of the gate, power singularity at the order of $r^{-1/2}$ at the side edges of the gate and a stronger power singularity, $r^{-3/2}$, at the bottom corner points of the gate. Inner region formulations near the side edges and the bottom line of the gate are quite a difficult task and not attempted in this paper.

CRediT authorship contribution statement

Elona Fetahu: Investigation, Validation, Formal analysis. **Olha Ivanyshyn Yaman:** Software, Writing – editing, Validation, Visualization. **Oguz Yilmaz:** Conceptualization, Methodology, Writing – original draft, Writing – reviewing, Supervision.

Declaration of competing interest

The authors declare that they have no known competing financial interests or personal relationships that could have appeared to influence the work reported in this paper.

Data availability

All the data are in the paper.

Acknowledgments

The problem studied in this paper was suggested by Prof. Alexander Korobkin, for which we are grateful. We are also grateful to Dr. Alessandro Iafrati for his comments on the numerical part of the paper. This investigation was carried out while the first author received a scholarship from Turkey Scholarships during her Ph.D. studies in Izmir Institute of Technology. This support is greatly acknowledged.

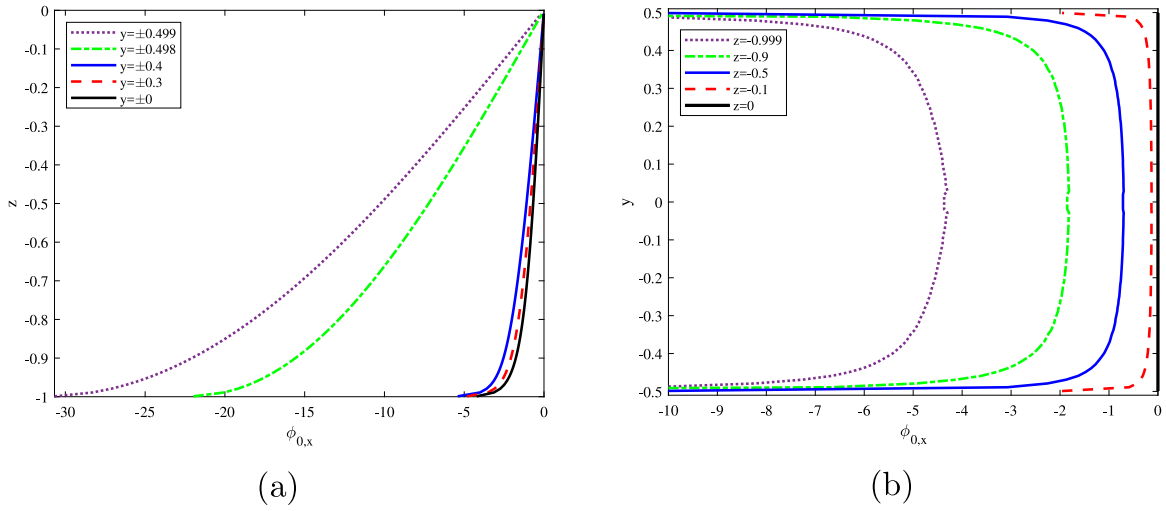

Fig. 6. Horizontal velocities for $b/H = 0.5$, $t = 1$ (a) along the vertical lines on the gate, (b) along the horizontal lines on the gate.

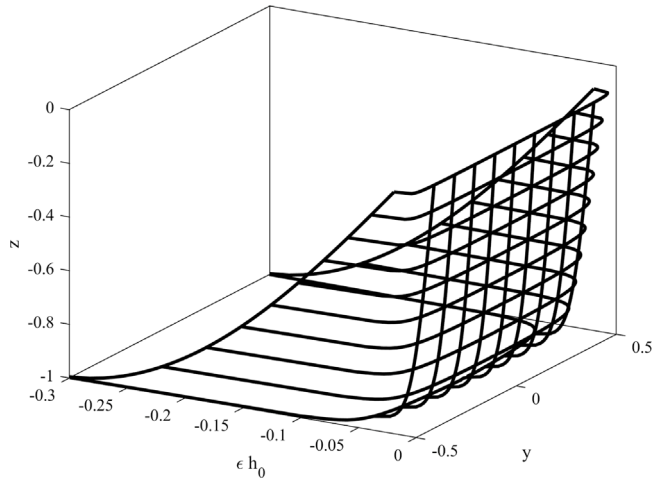

Fig. 7. Shape of the three dimensional free surface, $b/H = 0.5$, $\epsilon = 0.01$, $t = 1$.

References

Abramowitz, M., Stegun, I.A., 1970. Handbook of Mathematical Functions, ninth ed. National Bureau of Standards.

Battistin, D., Iafrati, A., 2003. Hydrodynamic loads during water entry of two dimensional and axisymmetric bodies. J. Fluids Struct. 17, 643-664.

Biscarini, C., Di Francesco, S., Manciola, P., 2010. CFD modelling approach for dam break flow studies. Hydrol. Earth Syst. Sci. 14, 705–718.

Brufau, P., Vazquez-Cendon, M.E., Garcia-Navarro, P., 2002. A numerical model for the flooding and drying of irregular domains. Int. J. Numer. Methods Fluids 39, 247–275.

Caboussat, A., Boyaval, S., Masserey, A., 2011. On the modeling and simulation of non-hydrostatic dam break flows. Comput. Vis. Sci. 14, 401–417.

Fetahu, E., Yilmaz, O., 2021. A three dimensional dam break flow: Small time behavior. Appl. Ocean Res. 110, 102583.

Iafrati, A., Korobkin, A.A., 2004. Initial stage of flat plate impact onto liquid free surface. Phys. Fluids 16 (7), 2214–2227.

Issakhov, A.A., Mussakulova, G., 2017. Numerical study for forecasting the dam break flooding flows impacts on different shaped obstacles. Int. J. Mech. 11, 273–280.

Issakhov, A., Zhandaulet, Y., Nogaeva, A., 2018. Numerical simulation of dam break flow for various forms of the obstacle by VOF method. Int. J. Multiphase Flow 109, 191–206.

Jha, A.K., Akiyama, J., Ura, M., 1995. First and second order flux difference splitting schemes for dam break flow. J. Hydraul. Eng. 121 (12), 877–884.

King, A.C., Needham, D.J., 1994. The initial development of a jet caused by fluid, body and free surface interaction. Part 1. A uniformly accelerating plate. J. Fluid Mech. 268, 89–101.

Korobkin, A.A., Pukhnachov, V.V., 1988. Initial stage of water impact. Annu. Rev. Fluid Mech. 20 (1), 169–185.

Korobkin, A., Yilmaz, O., 2009. The initial stage of dam break flow. J. Eng. Math. 63, 293–308.

Larocque, L.A., Imran, J., Chaudhry, M.H., 2013. 3D numerical simulation of partial breach dam-break flow using the LES and $k-\epsilon$ turbulence models. J. Hydraul. Res. 51 (2), 145–157.

Morse, P.M., Feshbach, H., 1953. Methods of Theoretical Physics, first ed. McGraw-Hill Book Company..

Penney, W.G., Thornhill, C.K., Fox, L., Goodwin, E.T., 1952. Part III. The dispersion, under gravity, of a column of fluid supported on a rigid horizontal plane. Philos. Trans. R. Soc. Lond. Ser. A, Math. Phys. Sci. vol. 244 (882), 285–311.

Pohle, F., 1950. The Lagrangian Equations of Hydrodynamics: Solutions Which are Analytic Functions of Time School (Ph.D. thesis). New York University.

Renzi, E., Dias, F., 2013. Hydrodynamics of the oscillating wave surge converter in the open ocean. Eur. J. Mech. B Fluids 41, 1–10.

Stansby, P.K., Chegini, A., Barnes, T.C.D., 1998. The initial stages of dam-break flow. J. Fluid Mech. 374, 407–424.

Stoker, J.J., 1957, Water waves, Interscience Publishers Inc, New York, USA.

Yilmaz, O., Korobkin, A., Iafrati, A., 2013. The initial stage of dam break flow of two immiscible fluids, linear analysis of global flow. Appl. Ocean Res. 42, 60–69.

Zhou, J.G., Causon, D.M., Mingham, C.G., Ingram, D.M., 2004. Numerical prediction of dam-break flows in general geometries with complex bed topography. J. Hydraul. Eng. 130 (4), 332–340.